Multiphoton fragmentation of H_2^+ and D_2^+ with coherent and incoherent fields

S. Miret-Artes
Instituto de Matemáticas y Física Fundamental, Consejo Superior de Investigaciones Científicas, Serrano 123, 28006 Madrid, Spain

David A. Micha
Quantum Theory Project, University of Florida, Gainesville, Florida 32611
(Received 1 July 1994)

A theory of molecular photofragmentation is developed for coherent and incoherent light and for the case where dissociation lifetimes of field-induced resonances are shorter than pulse lengths. Using a mixed representation for the transition operator (a description of the initial state of the field with the coherent representation and of the final state with the number representation), we show how observables are modified at different field regimes by Poisson distributions. Applications to H_2^+ and D_2^+ are presented and discussed. They include line shapes and final distributions of kinetic energies for weak, intermediate, and strong fields. Results show that the interference of resonance states plays an important role even after averages over the field phases have been carried out to account for incoherent effects.

PACS number(s): 42.50.Hz, 33.80.Wz, 33.80.Gj

I. INTRODUCTION

The multiphoton dissociation of very simple molecular ions (such as H_2^+ and D_2^+) using intense radiation fields is being actively investigated [1–12]. New effects and mechanisms are being predicted and observed, such as above-threshold dissociation (ATD), bond softening (BS), vibrational trapping (VT), etc., and an appropriate theoretical framework is being developed to understand these new phenomena. It is well known that lasers operating above their thresholds are described by a superposition of occupation number states or Fock states; that is, they are not in a pure photon number state. The greater the average occupation number, the closer is the approach to the one in terms of a classical electromagnetic field. Thus, phenomena involving photon absorption and stimulated emission have been described by a semiclassical time dependent Hamiltonian with a uniform classical electric field in the dipole approximation. This representation combined with an expansion in molecular states leads to a time independent description of photodissociation in terms of Floquet blocks [13]. It has the advantage of providing simple and intuitive explanations of those phenomena, and leads to close-coupling (CC) equations easily solvable. Several methods for solving such CC equations can be found in the literature [13,4,5,14]. Wave-packet propagation methods [3,6] have also been applied to the study of molecular photodissociation, and a collisional time correlation function approach to the interaction of photons with polyatomic systems has been proposed for general laser sources [15].

Theoretical treatments in this area have largely used the number representation although some recent studies have introduced the coherent-state representation [16]. This representation was considered some time ago [17,18] for weak fields. Very recently [9], we have also employed the coherent representation for treating this photodissociation dynamics. It was shown that the statistical distribution of both the amplitude and the phase of the field modes plays a very important role in the total photodissociation probabilities [9]. Our aim in this paper is to extend our treatment to the study of other observables (such as absorption cross sections, resonance widths and shapes, and final kinetic-energy distributions) and to see how Poisson averages arising in the coherent representation [19,20] modify them when going from weak-field to very strong-field regimes. Only a single mode of the field has been considered in order to simplify the discussion; this approach is also suitable when the modes of the field are independent.

Our starting point is the theory developed in Ref. [5]. It is a generalization of the artificial channel method [21] for the calculation of direct photodissociation cross sections at weak-field regimes. For radiative lifetimes of field-induced resonances shorter than pulse lengths, the total photodissociation probability for a transition from an initial bound-electronic state to a continuum electronic state is expressed in terms of the corresponding transition matrix element [22]. This element is usually given in the number representation and we obtain it from the CC equations in the semiclassical limit. The next step is to pass to a mixed representation of this element, that is, the final state of the field is described in the number representation and the initial state of the field in the coherent representation. The Poisson averages of the observables come from the average over the initial phase of the field. This approach can be supported by the following arguments. From an experimental point of view, intense 100 ps or 160 fs laser pulses [2] have been used in the domain of optical frequencies. For these conditions, the dynamics proceed in the presence of radiation since dissociation times are found to be shorter than pulse durations for the systems studied here. In other words, experiments are carried out under continuous wave field conditions. Moreover, in the optical domain, phase measurements are difficult [20] and pulses are well represented by coherent signals with no knowledge, however, of the initial phase (the field is said to be in a random-phase-coherent state). The final state of the field is given in the number representation because we know the relative number of photons absorbed (or $\Delta n = n_i - n_f$) from the experimental measurement of the final kinetic energies of

the products and therefore the sum over the final number of photons can be performed easily.

Finally, the phenomenon of isotope separation is also studied within this formalism since at very strong-field regimes the overlapping of resonances is important in the separation and a study in terms of cross sections or branching ratios should be more adequate than one in terms of isolated resonances [10].

II. THEORETICAL FORMALISM

A. Coupled equations

1. Total Hamiltonian, interaction and states

In our model for the molecular photodissociation, we consider only two electronic states of the system, denoted by $|g\rangle$ (ground electronic state) and $|d\rangle$ (dissociative excited electronic state). The corresponding internal molecular states will be labeled by $|g,v\rangle$ and $|d,\varepsilon\rangle$, respectively; v and ε are the vibrational quantum number and the relative kinetic energy. For simplicity, any change in the rotational quantum number due to the interaction with the field is neglected (J-conserving approximation). As concerns the radiation field, its Hamiltonian will be expressed in terms of only one mode, the active mode. This is again done to simplify the discussion. The e.m. field state will be characterized either by its photon occupation number $|n\rangle$ and energy $n\hbar\omega$ or by a coherent-state $|\alpha\rangle$ which is defined as a normalized eigenstate of the annihilation operator a; the corresponding eigenvalue is, in general, a complex number $\alpha=|\alpha|\exp(i\phi)$, where $|\alpha|$ and ϕ represent the amplitude and phase of one mode of the field, respectively. The transformation between both representations is given by [20(a)]

$$\langle n|\alpha\rangle=\frac{\exp(-|\alpha|^2/2)\alpha^n}{\sqrt{n!}}, \tag{1}$$

so that

$$|\langle n|\alpha\rangle|^2=\frac{\exp(-|\alpha|^2)|\alpha|^{2n}}{n!} \tag{2}$$

is a Poisson distribution of field intensities and is interpretable as the probability of finding n photons in a coherent-state $|\alpha\rangle$. The matter-field interaction will be considered within the dipole approximation. In practice, as will be shown later, the radiation-field gauge will be employed in our calculations. Thus, we have for the total Hamiltonian

$$H=H_m+H_{\rm rad}+V, \tag{3}$$

with

$$H_m=\sum_{s=g,d}|s\rangle[T_R+V_{ss}(R)]\langle s|, \tag{4}$$

$$H_{\rm rad}=\hbar\omega(a^\dagger a+1/2), \tag{5}$$

and

$$V=-\boldsymbol{\mu}(R)\cdot\mathscr{E}=-i\mu(R)\left(\frac{\hbar\omega}{2\epsilon_0 L^3}\right)^{1/2}(a-a^\dagger). \tag{6}$$

Here T_R is the kinetic-energy operator as a function of the R variable, the dissociative coordinate. The functions $V_{gg}(R)$ and $V_{dd}(R)$ are the potential energies for the $|g\rangle$ and $|d\rangle$ states; a and $a^\dagger$ are the photon annihilation and creation operators, respectively; ω is the laser frequency; ϵ_0 is the electric permittivity in the vacuum, and L^3 is the volume of the cavity. In Eq. (6) it has been assumed that the electric field $\mathscr{E}$ is linearly polarized and the dipole moment $\boldsymbol{\mu}$ of the molecule is parallel to this direction [2] and a function of the internuclear distance. The unperturbed states of $H_0=H_m+H_{\rm rad}$ are described by direct products of a molecular state and a field state. The following notation will be used: $|s,n\rangle\equiv|s\rangle|n\rangle$, where the index s is a collective one for describing the molecular states.

Starting from the Schrödinger equation

$$H|\Psi\rangle=E|\Psi\rangle, \tag{7}$$

where

$$E=n_i\hbar\omega+E_g^{\rm eq}+E_v=n_f\hbar\omega+E_d+\varepsilon, \tag{8}$$

with $E_d=\lim V_{dd}(R)$ for $R\to\infty$, and $E_g^{\rm eq}=V_{gg}(R_{\rm eq})$, we are going to express the equations governing this problem using two different representations: the photon-number and the coherent-state representations.

2. Photon-number representation

If the total wave function $|\Psi\rangle$ is expanded in the photon-number states according to

$$|\Psi\rangle=\sum_{n=0}^{\infty}|n\rangle\langle n|\Psi\rangle \tag{9}$$

and the coefficient functions are further expanded in the electronic states,

$$\langle n|\Psi\rangle=|g\rangle|g,v,n\rangle+|d\rangle|d,\varepsilon,n\rangle. \tag{10}$$

We substitute it in Eq. (7), after premultiplying first by $\langle m|$ and then by $\langle g|$ and $\langle d|$, to get the following close-coupling (CC) equations:

$$[T_R+V_{gg}(R)+m\hbar\omega-E]|g,v,m\rangle-i(\mathscr{E}_0/2)\mu_{dg}(R)\times[\sqrt{m+1}|d,\varepsilon,m+1\rangle-\sqrt{m-1}|d,\varepsilon,m-1\rangle]=0, \tag{11}$$

$$[T_R+V_{dd}(R)+(m+1)\hbar\omega-E]|d,\varepsilon,m+1\rangle-i(\mathscr{E}_0/2)\mu_{dg}(R)[\sqrt{m+2}|g,v,m+2\rangle-\sqrt{m}|g,v,m\rangle]=0, \tag{12}$$

where the orthogonality condition has been used for the field and electronic states; $\mu_{dg}(R)$ the corresponding transition dipole moment and $\mathscr{E}_0$ the amplitude of the field given by

$$\mathscr{E}_0=\left(\frac{2I}{\epsilon_0 c}\right)^{1/2}, \tag{13}$$

with

$$I=\frac{c\hbar\omega}{L^3}, \tag{14}$$

c being the light speed and I the intensity of the field. With a convenient election of the origin of energy, the zero point energy is not included.

Both absorption and stimulated and spontaneous emission appear in Eqs. (11) and (12) because a quantized radiation field is employed in this representation. However, as is very well known, the nature of both emissions is different. In our calculations we will be using a classical electric field and therefore will not be describing spontaneous emission, which appears only after quantizing the electromagnetic field. For our purposes, this is not a problem because we are treating photodissociation in strong fields (nearly monochromatic with small fluctuations) and spontaneous emission is negligible.

We must solve the CC equations with the proper boundary conditions, to obtain bound vibrational states $|gv\rangle$ in the ground electronic state and scattering states $|d\varepsilon\rangle$ in the dissociative state. The equations can describe multiphoton processes because from their solution we can calculate the matrix elements of the transition operator, $\langle d,\varepsilon,n_f|T|g,v,n_i\rangle$, where n_f and n_i denote the final and initial number of photons of the field, via the collisional S matrix. The structure of these CC equations is very typical and can be seen as formed by blocks (Floquet blocks) [13] of dressed electronic states corresponding to different photon occupation numbers, each block containing two dressed states (for n and $n+1$ photons). When only the resonant transition block is considered (a set of two CC equations), it leads to the rotating wave approximation (RWA). Obviously, the number of Floquet blocks (or CC equations) to be solved increases dramatically with the intensity of the laser. For these cases, an isolated resonance approximation (IRA) is no longer applicable and instead absorption cross sections or photodissociation probabilities (or branching ratios) must be calculated.

3. Coherent-state representation

Lasers operating above their thresholds are described by a superposition of Fock states, that is, they are not in a pure photon-number state. For these cases, the statistical distribution of both the amplitude and the phase of the field can play a very important role in the final results. To study their roles, it is advantageous to begin with the coherent-state representation of the field. Again, since the modes of the field are independent only a single mode will be under discussion. Two different approaches can be envisaged at this level. The first one was derived in Ref. [18] within the RWA; the CC equations were given in terms of the field variables after the quantum-mechanical operators a and $a^\dagger$ were replaced by c numbers. They furnished simple analytical expressions for the transition probabilities. This approach however seems cumbersome for strong fields. Our recent approach [9] is based on a change of representation. We can maintain all the advantages of a description in a number representation and, after passing to the coherent representation, a more direct comparison with the experimental results can be done. Thus, the transition matrix elements can be written using completeness of the number states as,

$$\langle d,\varepsilon,\beta|T|g,v,\alpha\rangle=\sum_{n,m=0}^{\infty}\langle\beta|m\rangle\langle d,\varepsilon,m|T|g,v,n\rangle\langle n|\alpha\rangle, \tag{15}$$

or as

$$\langle d,\varepsilon,m|T|g,v,\alpha\rangle=\sum_{n=0}^{\infty}\langle d,\varepsilon,m|T|g,v,n\rangle\langle n|\alpha\rangle, \tag{16}$$

since, in some cases, it can be useful to get a mixed representation; that is, to represent the initial state of the field by the coherent representation and the final state of the field by the number representation.

4. The semiclassical approach

When strong fields are involved in the experiments, it is quite natural to ignore the quantum description of the field and to treat it classically by assuming a uniform electric field $\mathscr{E}_0\cos(\omega t+\phi)$. In this context, the total Hamiltonian is time dependent according to

$$H=H_m+\boldsymbol{\mu}\cdot\mathscr{E}_0\cos(\omega t+\phi), \tag{17}$$

so that H is periodic in t. We develop the total wave function in a Fourier series

$$\Psi(q,R,t)=e^{-iEt/\hbar}\sum_n\Phi_n(q,R)e^{in\omega t}, \tag{18}$$

with

$$\Phi_n(q,R)=\psi_g(q;R)\chi_{g,v,n}(R)+\psi_d(q;R)\chi_{d,\epsilon,n}(R), \tag{19}$$

where the $\psi(q;R)$ functions represent the electronic wave functions for the two electronic states depending on electronic coordinates (q) and the $\chi(R)$ functions are the nuclear wave functions with a subindex n noting the dependence on the field states. Then, by substitution of Eqs. (17)–(19) in the time dependent Schrödinger equation

$$i\hbar\frac{\partial\Psi(q,R,t)}{\partial t}=H\Psi(q,R,t) \tag{20}$$

and after integration over t, premultiplication first by $\psi_g^*(q;R)$ and next by $\psi_d^*(q;R)$ and again integration over the electronic coordinates, we get the following semiclassical coupled (SC) equations,

$$[T_R+V_{gg}(R)+m\hbar\omega-E]\chi_{g,v,m}(R)-(\mathscr{E}_0/2)\mu_{dg}(R)\times[\chi_{d,\varepsilon,m+1}(R)+\chi_{d,\varepsilon,m-1}(R)]=0, \tag{21}$$

$$[T_R+V_{dd}(R)+(m+1)\hbar\omega-E]\chi_{d,\varepsilon,m+1}(R)-(\mathscr{E}_0/2)\mu_{dg}(R)[\chi_{g,v,m+2}(R)+\chi_{g,v,m}(R)]=0. \tag{22}$$

These SC equations have a very similar structure to the CC equations, Eqs. (11) and (12); the two sets agree for $m\gg1$. The integration of these equations can be done in coordinate space, and very efficient algorithms can be applied to obtain the solutions $\chi_{g,v,m}$ and $\chi_{d,\varepsilon,m}$. Information concerning the

transition matrix elements, $\langle d,\varepsilon,n_f|T|g,v,n_i\rangle_{\rm SC}$ is obtained from such solutions [21]. Moreover, to a very good approximation, the transition matrix elements in Eqs. (15) or (16) can be replaced by the corresponding semiclassical ones.

B. Strong-field regime: Transition probabilities and kinetic-energy distribution

For dissociation times shorter than pulse lengths, we can obtain the total photodissociation probability for a transition from an initial bound-state $|g,v,n_i\rangle$ to a continuum state $|d,\varepsilon,n_f\rangle$ as [5]

$$P^{\rm coh}_{dn_f;gvn_i}(\omega,I)=\int d\varepsilon\frac{|\langle d,\varepsilon,n_f|T|g,v,n_i\rangle|^2}{(\varepsilon-E_{gv}-n_i\hbar\omega)^2}\,, \tag{23}$$

where we have denoted to the left that the CC probabilities include coherence effects. The quantity in the integral can be obtained directly by solving the CC equations and it is related to an S matrix in a very simple way [5]. We prefer to solve the SC equations instead of the CC equations and therefore the square matrix elements of the T operator have to be replaced by their semiclassical counterparts. At very high intensities of the field, this replacement is very good.

The SC probabilities can also be written as

$$P^{\rm coh}_{dn_f,gvn_i}(\omega,I)_{\rm SC}=P^{{\rm coh},\Delta n}_{d,gv}(\omega,I), \tag{24}$$

with I giving the average number of initial photons $\bar{n}_i$. Usually, the initial and final number of photons is not known in the experiment; only the difference $\Delta n=n_i-n_f$ is known. We could start with a coherent description for the initial state of the field and a number representation for the final state. This mixed representation is useful for describing the photodissociation. Obviously, our final formula has to be summed over n_f and averaged over the initial phase of the field since it is usually not known (for a random-phase-coherent field). This averaging procedure gives us a Poisson distribution insofar, from Eq. (16) with $\alpha=|\alpha|\exp(i\phi)$,

$$\begin{aligned}\langle|T_{d\varepsilon n_f;gv|\alpha_i|}|^2\rangle&=\frac{1}{2\pi}\int_0^{2\pi}d\phi_i|\langle d,\varepsilon,n_f|T|g,v,\alpha_i\rangle|^2,\\&=\sum_{n_i=0}^{\infty}|\langle n_i|\alpha_i\rangle|^2|\langle d,\varepsilon,n_f|T|g,v,n_i\rangle|^2.\end{aligned} \tag{25}$$

With these conditions, we get photodissociation probabilities for incoherent light. Thus, we have from Eqs. (23)–(25) that, in the SC approximation,

$$P^{\rm inc}_{d;gv|\alpha_i|}(\omega,I)=\sum_{n_f,n_i=0}^{\infty}P^{\rm coh}_{dn_f;gvn_i}(\omega,I)|\langle n_i|\alpha_i\rangle|^2, \tag{26}$$

gives

$$P^{\rm inc}_{d;gv|\alpha_i|}(\omega,I)=\sum_{\Delta n\geq 1}P^{{\rm coh},\Delta n}_{d;gv}(\omega,I)\sum_{n_i\geq\Delta n}|\langle n_i|\alpha_i\rangle|^2, \tag{27}$$

with

$$\sum_{n_i\geq\Delta n}|\langle n_i|\alpha_i\rangle|^2=1-\sum_{n_i<\Delta n}|\langle n_i|\alpha_i\rangle|^2, \tag{28}$$

where we have used the completeness of the $\{|n_i\rangle\}$ set. This quantity $P^{\rm inc}_{d;gv|\alpha_i|}(\omega,I)$ is the one to be compared to experimental results with incoherent light generated with very short pulses (for example, in the experiments with intense laser fields used in Ref. [2]). It depends on the value of $|\alpha_i|$, which can be extracted by fitting the intensity of the field as [20(b)]

$$I=\frac{c\hbar\omega}{L^3}|\alpha_i|^2. \tag{29}$$

As regards the kinetic-energy distribution of the fragments it has been shown in Ref. [5] that

$$\begin{aligned}&\langle d,\varepsilon,n_f|T|g,v,n_i\rangle\\&\quad=(\varepsilon-E_{gv}-n_i\hbar\omega)\sum_K\frac{\langle d,\varepsilon,n_f|\tau|K\rangle\langle K|g,v,n_i\rangle}{\varepsilon-E_K+i\Gamma_K/2}\,,\end{aligned} \tag{30}$$

with τ a reduced T-matrix operator related to the projection operators over all continuum states connecting the $|K\rangle$ states to the physical final continuum states; $|K\rangle$ labels the field-induced resonances with complex energies $E_K-i\Gamma_K/2$; that is, they are the eigenstates of an optical potential and represent the dressed states of the problem. The overlaps $\langle K|g,v,n_i\rangle$ describe the preparation of the initial state. According to Eq. (25), the kinetic-energy distribution for incoherent light is also weighted by a Poisson distribution and gives the incoherent cross section

$$\begin{aligned}\Sigma^{\rm inc}_{d;gv|\alpha_i|}(\varepsilon;\omega,I)=\frac{2\pi\omega}{I}\sum_{n_f,n_i=0}^{\infty}|\langle n_i|\alpha_i\rangle|^2(\varepsilon-E_{gv}-n_i\hbar\omega)^2\\\times\left|\sum_K\frac{\langle d,\varepsilon,n_f|\tau|K\rangle\langle K|g,v,n_i\rangle}{\varepsilon-E_K+i\Gamma_K/2}\right|^2,\end{aligned} \tag{31}$$

where we have multiplied Eq. (25) by the factor $2\pi/(\hbar F_i)$ with F_i being the incident light flux $(I/\hbar\omega)$. The sum over n_f has been included since usually the number of photons remaining in the field is not known. This quantity is the one to be compared with the experimental kinetic-energy distributions. Depending on the intensity of the field, the number of $|K\rangle$ states contributing to the sum over K will increase dramatically and therefore this distribution will display a strong interference structure. Another interesting aspect of this equation comes from the sum over n_f and average over n_i. An interference structure is obtained for each of their values and is different for each Δn.

All of these general results can be better understood in the weak-field regime which is the subject of Sec. II C.

C. Weak-field regime

By starting from Eq. (16) in the form

$$\langle d,\varepsilon,n_f|T|g,v,\alpha_i\rangle=\sum_{n_i=0}^{\infty}\langle d,\varepsilon,n_f|T|g,v,n_i\rangle\langle n_i|\alpha_i\rangle, \quad (32)$$

and considering the first order in the perturbation series of the T operator, $T\simeq V$, we can directly obtain the width of the quasibound state (g,v) for this photodissociation process. Thus, by including the sum over n_f and average over n_i and after integration over the initial phase, we get the incoherent width for this level,

$$\Gamma^{\rm inc}_{d,gv|\alpha_i|}(\omega,I)=\sum_{n_f,n_i=0}^{\infty}\Gamma^{\rm coh}_{dn_f,gvn_i}(\omega,I)|\langle n_i|\alpha_i\rangle|^2, \quad (33)$$

with

$$\Gamma^{\rm coh}_{dn_f,gvn_i}(\omega,I)=2\pi|\langle d,\varepsilon,n_f|V|g,v,n_i\rangle|^2 \times\delta(E_d+n_f\hbar\omega+\varepsilon-E_{gv}-n_i\hbar\omega). \quad (34)$$

The δ function is a reminder that the coherent width is calculated *on-energy shell*. From the knowledge of that incoherent width, we could also define an incoherent photoabsorption line shape by means of the standard definition, that is, the transition probability per unit time and incident flux,

$$\sigma^{\rm inc}_{d,gv|\alpha_i|}(\omega)=\omega\frac{\Gamma^{\rm inc}_{d,gv|\alpha_i|}(\omega,I)}{I}. \quad (35)$$

The functional dependence of the cross section on I has disappeared because to first order the incoherent width is linear with the intensity and this is canceled by the denominator.

At weak fields, direct photodissociation proceeds mainly by absorption of a single photon (in this case, $\Delta n=n_i-n_f=1$). Therefore, from Eq. (33), arguing as for Eq. (27)

$$\Gamma^{\rm inc}_{d,gv|\alpha_i|}(\omega,I)=\Gamma^{\rm coh,1}_{d,gv}(\omega,I)(1-e^{-|\alpha_i|^2}), \quad (36)$$

and a similar expression follows for the absorption line shape

$$\sigma^{\rm inc}_{d,gv|\alpha_i|}(\omega)=\omega\frac{\Gamma^{\rm coh,1}_{d,gv}(\omega,I)}{I}(1-e^{-|\alpha_i|^2}), \quad (37)$$

where $\Gamma^{\rm coh,1}_{d,gv}(\omega,I)$ is the value for the coherent width for $\Delta n=1$. Equations (36) and (37) show that these observables are dependent on the square amplitude $|\alpha_i|^2$ of the field. We could use these formulae to fit the experimental values and hence to obtain through Eq. (29) the cavity volume L^3. In the derivation of the two last equations, spontaneous emission has not been taken into account.

Concerning resonance line shapes, we could begin with the full expression for the T-operator $T=V+VGV$ where G is the resolvent operator for the total Hamiltonian H. At weak fields, the transition matrix element for $(g,v,n_i)\rightarrow(d,\varepsilon,n_f)$ is given by

$$\langle d,\varepsilon,n_f|T|g,v,n_i\rangle=(\varepsilon-E_{gv}-n_i\hbar\omega)\frac{\langle d,\varepsilon,n_f|V|g,v,n_i\rangle}{\varepsilon-\bar{E}_{gvn_i}+i\Gamma^{\rm coh}_{dn_f,gvn_i}/2}. \quad (38)$$

This expression can be deduced from Eq. (30) in the weak-coupling limit, where the IRA holds, substituting $|K\rangle\rightarrow|g,v,n_i\rangle$, $\Gamma_K\rightarrow\Gamma^{\rm coh}_{gvn_i}$, $E_K\rightarrow\bar{E}_{gvn_i}=E_{gv}+n_i\hbar\omega+\Delta_{gvn_i}$ (where Δ is the energy shift of the level), $\tau\rightarrow V$, and observing that the sum over K is reduced to only one term.

In these conditions, Eq. (31) can be rewritten as

$$\Sigma^{\rm inc}_{d;gv|\alpha_i|}(\varepsilon;\omega,I)=\frac{2\pi\omega}{I}\sum_{n_f,n_i=0}^{\infty}|\langle n_i|\alpha_i\rangle|^2(\varepsilon-E_{gv}-n_i\hbar\omega)^2 \times\frac{|\langle d,\varepsilon,n_f|V|g,v,n_i\rangle|^2}{(\varepsilon-\bar{E}_{gvn_i})^2+(\Gamma^{\rm coh}_{gvn_i})^2/4}, \quad (39)$$

where the profile for a resonance is the result of an incoherent sum of profiles (in general, with different signatures) weighted by a Poisson distribution. In the case $\Delta n=1$ (absorption of a single photon) and due to the fact that all the profiles are in terms of ε, the relative kinetic energy, Eq. (39) is transformed into

$$\Sigma^{\rm inc}_{d;gv|\alpha_i|}(\varepsilon;\omega,I)=\frac{2\pi\omega}{I}(\varepsilon-E_{gv}-\hbar\omega)^2 \times\frac{|\langle d,\varepsilon,0|V|g,v,1\rangle|^2}{(\varepsilon-\bar{E}_{gvn_i})^2+(\Gamma^{\rm coh,1}_{gvn_i})^2/4} \times(1-e^{-|\alpha_i|^2}), \quad (40)$$

where we find again the same factor as in Eqs. (36) and (37).

III. RESULTS AND DISCUSSION

A. Field regimes

Before going on to show the results obtained for the H_2^+ and D_2^+ ions, it is important to characterize the field regime. The simplest criterion is based on the Rabi frequency. For the photodissociation process studied here, the radiative Rabi frequency (or electronic transition frequency) ω_{dg} is

$$[\omega_{dg}(R)\ \ ({\rm cm})^{-1})]=1.17\times10^{-3}[\mu_{dg}(R)\ \ ({\rm a.u.})] \times[I\ \ ({\rm W/cm^2})]^{1/2}, \quad (41)$$

which is to be compared to the vibrational frequency of the molecular system. Its value at equilibrium is obtained from $\mu_{dg}(R_{\rm eq})=1.07ea_0$. When ω_{dg} is much less than a vibrational frequency we are in a weak-field regime (WF); if it is of the same order, we speak about an intermediate regime (IF) and if it is larger or much larger, the corresponding regime is strong or very strong (SF or VSF). Thus we can have an idea of how many vibrational states the light is exciting. Obviously, the wavelength (λ) of light (or its excita-

TABLE I. Classification of the field regime for several intensities at $\lambda = 3296.7$ A ($\lambda^{-1} = 3.0309\,4 \times 10^4$ cm^{-1}) and for the first vibrational states of H_2^+. The molecular parameters are: $\omega_v = 2358.571$ cm^{-1}, $\gamma = 19.099$ cm^{-1} (anharmonicity), and $D = 22\,522.852$ cm^{-1} (well depth). The Rabi frequency ω_{dg} was obtained at the equilibrium distance of H_2^+, $R_e = 2.0$ a.u., and with $\mu_{dg}(R_e) = 1.07 e a_0$. The values of $|\alpha_i|^2$ have been obtained taking as reference $|\alpha_i|^2 \simeq 9.0$ for $I = 2.45 \times 10^{13}$ W/cm^2.

I (W/cm^2)	ω_{dg} (cm^{-1})	Regime	$\lvert\alpha_i\rvert^2$
3.52×10^6	1.9225×10^1	WF	1.29×10^{-6}
3.52×10^{10}	1.9225×10^3	WF	1.29×10^{-2}
3.52×10^{12}	1.9225×10^4	IF	1.29
3.52×10^{14}	1.9225×10^5	SF	1.29×10^2
3.52×10^{16}	1.9225×10^6	VSF	1.29×10^2

tion energy) must also be considered. If the excitation energy is of the same order of magnitude as the well depth of the interaction potential of the ions, the number of Floquet blocks to be included in the calculations has to be much larger than when the excitation energy is small. Notice that nothing is said about the laser source: we may be dealing with a continuous-wave laser or a pulse with a given duration and where a distribution of intensities is present. Summing up, in each case we could construct a table to establish the different regimes as functions of the intensity for a given wavelength and initial state; this is done in Table I. At WF, linear effects of the field are present and are related to energy-shell contributions. Also, Fermi's "golden rule" and IRA hold. At IF, nonlinear effects of the field begin to appear, related to off-energy-shell contributions, and nonperturbative treatments have to be implemented. The RWA still holds and the IRA begins to fail. For SF and VSF, the IRA and RWA are no longer applicable; new nonlinear effects are predicted and observed in this regime such as above threshold dissociation (ATD), bond softening (BS), or vibrational trapping (VT), etc. Concerning the formal intensity law for multiphoton transitions, and within a perturbative treatment, it is very easy to show that the n-photon transition probability is proportional to I^n. In our semiclassical formulation, it can be obtained from the number of open Floquet blocks needed for convergence; the closed Floquet blocks represent virtual processes (kinetic energies of the fragments are negative) and therefore they must not contribute to the power law of the intensity.

When a coherent representation of the field is used, the corresponding expressions are written in terms of the field magnitude $|\alpha_i|^2$. Since the value of the cavity volume is needed in Eq. (29), and this value is not usually known, we obtain it by fitting a theoretical result to an experimental one. This was done in Ref. [9] and a magnitude of $|\alpha_i|^2 \simeq 9.0$ for $\lambda = 329.7$ nm and $I = 2.45 \times 10^{13}$ W/cm^2 was calculated (a cavity volume of 633 Å^3 was obtained in this way). In these conditions, experimental observation and SC calculations show that the photodissociation dynamics proceeds mainly via the absorption of two photons (ATD mechanism). With this volume, we can calculate what $|\alpha_i|^2$ corresponds to each intensity. At a given intensity, the same $|\alpha_i|^2$ will be used in the calculations for different λ. We have listed in Table I the values of this quantity at several field regimes.

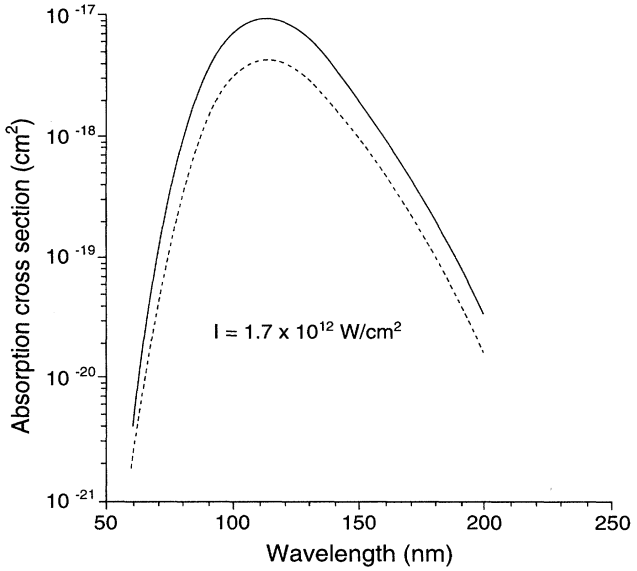

FIG. 1. Absorption cross section for the initial state ($v = 0, j = 1$) of H_2^+ at $I = 1.7 \times 10^{12}$ W/cm^2 using coherent light (solid line) and incoherent light (dashed line).

B. Incoherent light at WF and IF regimes

From inspection of Table I, we see that the magnitude $|\alpha_i|^2$ changes by several orders of magnitude when we pass from one field regime to another. At incoherent WF (for this system, below 10^{10} W/cm^2) and $\Delta n = 1$, the factor $(1 - e^{-|\alpha_i|^2})$ appearing in Eqs. (36), (37), and (40) is very small, meaning that when one averages over initial phases, the elimination of constructive phase interference leads to a very inefficient absorption process. If we move to the IF regime (between 10^{10} and 10^{13} W/cm^2), that factor is responsible for a strong attenuation of the different observables (widths, absorption line shapes, and resonance profiles). For example, at $I = 1.89 \times 10^{12}$ W/cm^2, the values of these observables are one half of their coherent values. Physically, this means that using incoherent light the maximum of absorption decreases dramatically but the lifetimes of resonances (inversely proportional to widths) increase. This behavior is illustrated in Fig. 1 where we display coherent (solid line) and incoherent (dashed line) photodissociation line shapes [Eq. (37)] for the $v = 0$, $j = 1$ level of the H_2^+ ground electronic state and using a laser of intensity 1.7×10^{12} W/cm^2. At this intensity we are in the limits of applicability of the RWA and Eq. (37) because neighboring resonance ($v = 1,2,3 \ldots ; j = 1$) begins to overlap.

As has been previously mentioned, in an IF regime, off-energy-shell contributions lead to nonlinear behavior of the dissociation rates as a function of intensity. From a numerical point of view, SC calculations involving one Floquet block have to be performed avoiding the use of perturbative expressions. For this goal, we have used a procedure based on a generalization of the artificial channel method. In particular, two artificial channels are introduced. The first one, a continuum channel, is added in order to transform the half-collision problem into a full collision one. The second one, a bound channel, plays the role of the true initial unperturbed molecular state, weakly coupled to the total molecular-field

manifold. In other words, this bound channel is introduced to select the initial state of the molecular system.

Another aspect requiring comment relates to the transition dipole used for the interaction. The electric-field gauge coupling (also called length form) expressed by Eq. (41) and the radiation-field gauge (or velocity form), which leads to an effective dipole

$$\bar{\mu}_{dg}(R)=\frac{V_{dd}(R)-V_{gg}(R)}{\hbar\omega}\,\mu_{dg}(R) \tag{42}$$

are both adequate, but in the IF and SF regimes the second gauge is more convenient because the coupling at large distances tends to zero.

The SC results are thus obtained through the following relation between the matrix elements of the T and S operators of collision theory

$$\frac{|\langle d,\varepsilon,n_f|T|g,v,n_i\rangle|^2}{(\varepsilon-E_{gv}-n_i\hbar\omega)^2}=A|\langle d,\varepsilon,n_f|S|a\rangle|^2, \tag{43}$$

where A is a constant determined by the calculations and $|a\rangle$ is the continuum artificial channel. With this condition, the total photodissociation probability, Eq. (23), is reduced to

$$P^{\mathrm{coh}}_{dn_f;gvn_i}(\omega,I)=A\int d\varepsilon|\langle d,\varepsilon,n_f|S|a\rangle|^2, \tag{44}$$

and from this we can obtain the incoherent probabilities given by Eq. (26).

From Eqs. (43) and (38), we observe that the matrix element $|\langle d,\varepsilon,n_f|S|a\rangle|^2$ displays a Lorentzian behavior in the IRA and WF regimes. Photodissociation proceeds via the first energetically accessible continuum state, it requires absorption of a single photon and yields the lowest relative kinetic energy, which means that the corresponding probability is nearly 1 (coherent result). However, the incoherent probability is again obtained multiplying by the $(1-e^{-|\alpha_i|^2})$ factor and equals a value less than 1 depending on the intensity of the laser. When we are considering an IF,

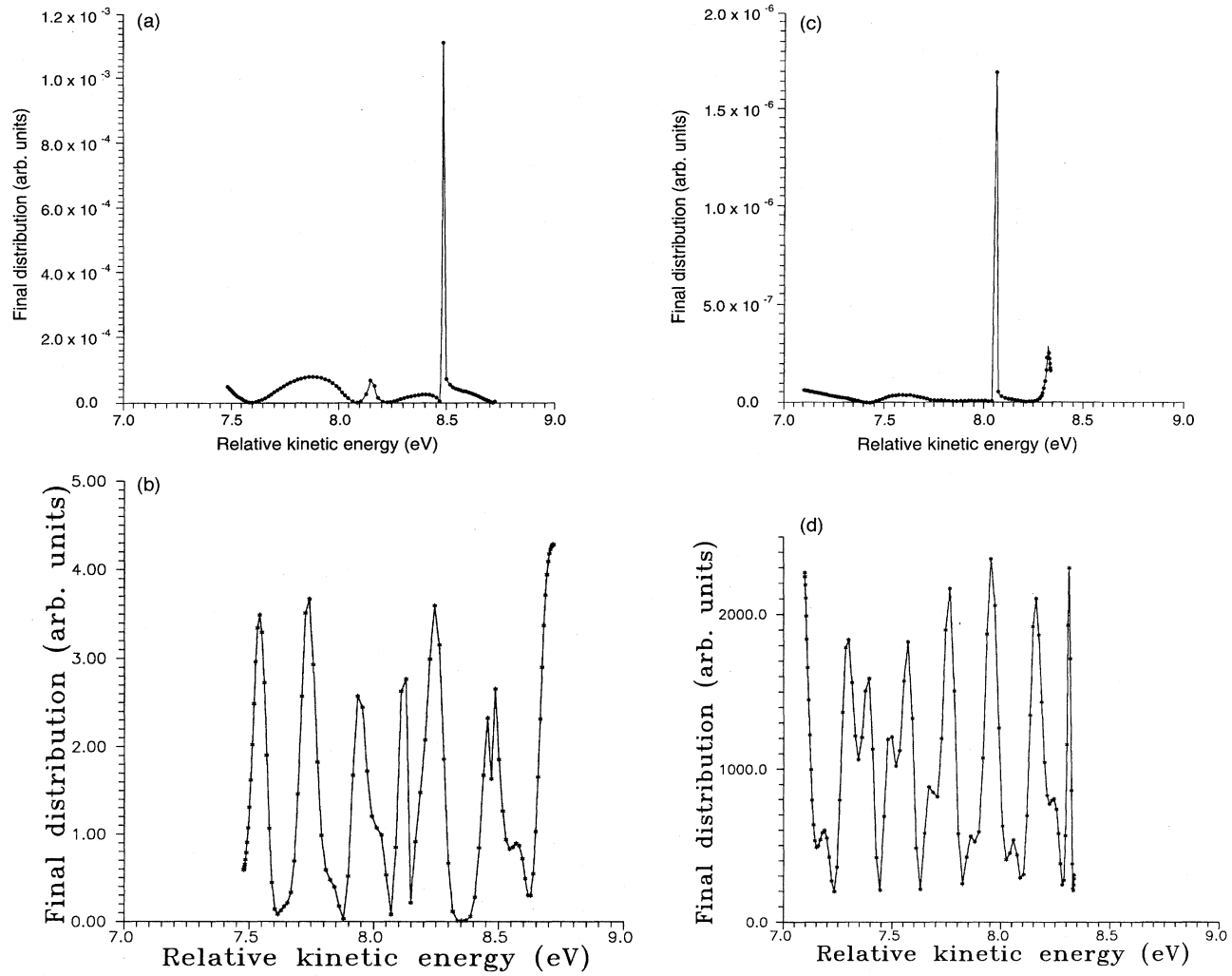

FIG. 2. Relative kinetic-energy distributions (in arbitrary units) at $I=1.25\times10^{13}$ W/cm^2 and $\lambda=120$ nm for H_2^+ $(v=2,j=1)$ corresponding to a SC calculation using (a) one Floquet block (RWA) and (b) five Floquet blocks. The same is plotted in the (c) and (d) panels for D_2^+ $(v=2,j=1)$, respectively.

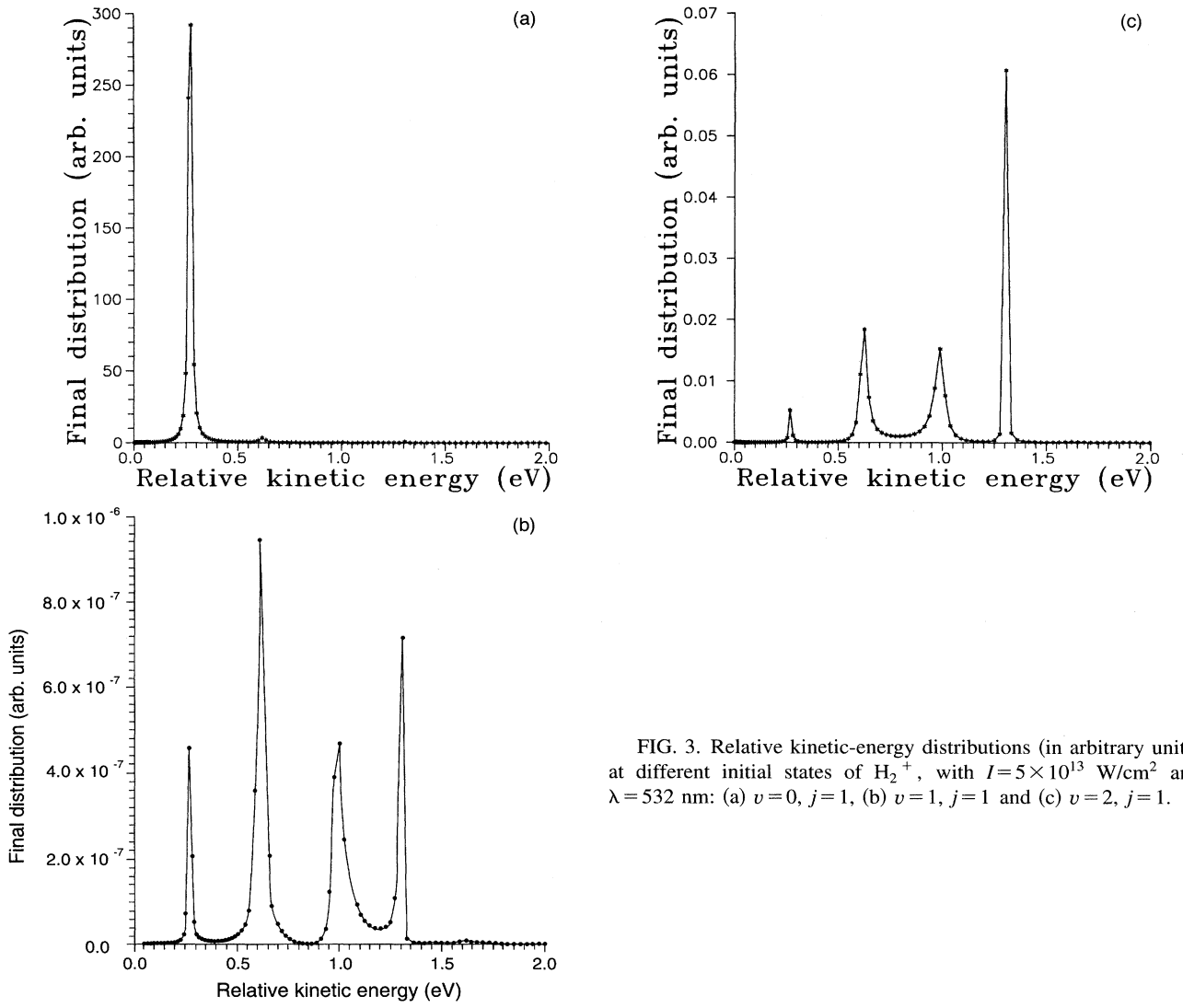

FIG. 3. Relative kinetic-energy distributions (in arbitrary units) at different initial states of H_2^+, with $I=5\times10^{13}$ W/cm^2 and $\lambda=532$ nm: (a) $v=0$, $j=1$, (b) $v=1$, $j=1$ and (c) $v=2$, $j=1$.

several continuum states are energetically accessible and each coherent probability is much less than 1. We have shown in a recent paper [9] that the SC probabilities may then differ enormously from phase-averaged or incoherent probabilities.

Experimentally, multiphoton fragmentation has been carried out by using intense 532 nm, 100 ps laser pulses. With a peak intensity below 50 TW/cm^2, the measured dissociation fraction is less than 0.2. In our SC calculations, for $I=1.7\times10^{12}$ W/cm^2, a dissociation fraction of about 0.2 and 0.1 is obtained for coherent and incoherent light.

C. Incoherent light at SF and VSF regimes

Very recently [10,11], the isotope effect in the H_2^+ and D_2^+ fragmentations by intense laser fields have shown some interesting results concerning two new photodissociation mechanisms of VT and BS. An isotope separation mechanism has been proposed in the first work [10] and, in the second one [11], a new interpretation of the BS mechanism has also been proposed as an alternative to that given originally [2]. In both cases, peak intensities of the pulses must be very high $10^{13}<I<10^{14}$ W/cm^2. In our experience, the RWA and IRA are not strictly applicable at these intensities even at wavelengths of about 120 nm, where the maximum of absorption is found [5]. It seems to us inappropriate to focus on the study of widths of isolated field-induced resonances insofar, after Eq. (31), relative kinetic-energy distributions show a strong mixing structure of such resonances. It should be better to treat isotope fragmentation using the theory developed here. Here, relative kinetic-energy distributions will be shown in order to illustrate these statements.

One of the intensities proposed for the isotope separation has been $I=1.25\times10^{13}$ W/cm^2 at $\lambda=120$ nm (around the maximum of absorption) and for an initial state of $v=2$ and $j=1$. In Figs. 2, we plot in arbitrary units the corresponding kinetic energy distributions for H_2^+ using only one Floquet block [Fig. 2(a)] and a converged calculation with five Floquet blocks [Fig. 2(b)], both obtained from Eq. (31) to include incoherence effects. The same is plotted for D_2^+ in Figs. 2(c) and 2(d), respectively. We observe that, for the

multiblock case, contributions from the one-photon absorption channel are the most important but that consideration of only the $(g,n_i=1)-(d,n_f=0)$ block is not adequate because the interference among the vibrational levels of the same g state is important at such an intensity and wavelength. In other words, the IRA does not hold in those conditions.

In Ref. [5] we showed that for the lowest vibrational level $(v=0,j=1)$, the corresponding profile was Lorentzian because the interference coming from the other vibrational levels and the other Floquet blocks was not important enough to noticeably disturb it (this is also in accordance with Ref. [16]). The higher vibrational levels produced Fano-type profiles, but important modifications of their line shapes and locations were observed leading to a complicated peak and dip pattern which cannot be easily correlated with the set of vibrational levels. Due to their strong coupling with light, they appeared to be nearly equally spaced; the anharmonicity was washed out by the field. Similar results are observed for H_2^+ and its isotope D_2^+ in the present converged calculations. In addition, here we are adding in accordance with Eq. (31), over weighted initial states and over final states, so that the patterns of final distributions have added complexity. Therefore, instead of analyzing widths of isolated field-induced resonances, we have found it is more appropriate to focus on global properties (for example, cross sections or branching ratios as in Ref. [11]). We find that these arguments remain valid after accounting for incoherence effects.

Finally, in Fig. 3, we show the same kind of distributions for H_2^+ with different initial states: (a) $(v=0,j=1)$ (b) $(v=1,j=1)$, and (c)$(v=2,j=1)$ for $\lambda=532$ nm and $I=50$ TW/cm^2 (for $v>2$, the contribution is five or more orders of magnitude smaller). Results were obtained from Eq. (31). The laser conditions correspond to the experimental ones. It must be noted that the initial state $(v=0,j=1)$ provides the main peak of this distribution; the other ones contribute very little since their values are smaller by several orders of magnitude, particularly for the initial $(v=1,j=1)$ state. Moreover, in Fig. 3(a), we observe that the peaks are positioned at 0.26, 0.64, 1.0, and 1.3 eV although their respective intensities are quite different. The two prominent peaks (at 0.26 and 1.3 eV) are separated by about $\hbar\omega/2=1.16$ eV and correspond to the two protons equally sharing the kinetic energy gained by absorbing a single photon. The intensity ratio between both peaks is 56. Similar features are observed in the experimental distribution [2]. In the mentioned experiments, the H_2^+ ion was formed in several vibrational states with different populations (from $v=0$ up to $v=6$) and therefore a direct comparison cannot be carried out. However, the first two peaks observed in the experimental kinetic-energy distribution can be regarded as coming from $v=0,j=1$ since this state gives the most important contribution.

IV. CONCLUSIONS

Starting with the description of diatomic photodissociation by quantized light, we have discussed the use of the number and coherent representations of the electromagnetic field, to account for the differences between dissociation for coherent and incoherent light sources.

Calculations for H_2^+ and D_2^+ were based on the solution of Floquet equations in a semiclassical limit for the field, valid for the high intensities (multiphoton phenomena) of interest.

The theory makes clear that large differences are to be expected in cross sections at weak-, intermediate-, and strong-field regimes. Magnitudes are very noticeably decreased by field phase averaging for weak and intermediate fields.

Details of the final distributions of kinetic energies of fragments, which are measurable properties, are found to depend on the interference of resonances at high intensities, with the interference effects remaining even after averaging over field phases to account for light incoherence. The calculated kinetic-energy distributions show features (spacings) present in the experimental distributions and confirm previous theoretical results within the number representation.

ACKNOWLEDGMENTS

The work of S.M.A. has been supported by CYCIT under Grant PB92-0053. The work of D.A.M. has been partly supported by the U.S. National Science Foundation.

[1] A. Giusti-Suzor, X. He, O. Atabek, and F. H. Mies, Phys. Rev. Lett. **64**, 515 (1990).
[2] P. H. Bucksbaum, A. Zavriyev, H. G. Muller, and D. W. Schumacher, Phys. Rev. Lett. **64**, 1883 (1990); Phys. Rev. A **42**, 5500 (1990); A. Zavriyev, P. H. Bucksbaum, J. Squier, and F. Saline, Phys. Rev. Lett. **70**, 1077 (1993).
[3] A. Giusti-Suzor and F. H. Mies, Phys. Rev. Lett. **68**, 3869 (1992).
[4] (a) X. He, O. Atabek, and A. Giusti-Suzor, Phys. Rev. A **38**, 5586 (1988); (b) **42**, 1585 (1990).
[5] S. Miret-Artes, O. Atabek, and A. D. Bandrauk, Phys. Rev. A **45**, 8056 (1992).
[6] G. Jolicard and O. Atabek, Phys. Rev. A **46**, 5845 (1992).
[7] M. Chrysos, O. Atabek, and R. Lefebvre, Phys. Rev. A **48**, 3855 (1993).
[8] E. E. Aubanel, A. Lonjusteau, and A. D. Bandrauk, Phys. Rev. A **48**, R4011 (1993).
[9] S. Miret-Artes and D. A. Micha, Phys. Rev. A **48**, R4059 (1993).
[10] O. Atabek, M. Chrysos, and R. Lefebvre, Phys. Rev. A **49**, R8 (1994).
[11] S. Miret-Artes and O. Atabek, Phys. Rev. A **49**, 1502 (1994).
[12] G. Yao and S. I. Chu, Phys. Rev. A **48**, 485 (1993).
[13] S. I. Chu, J. Chem. Phys. **75**, 2215 (1981).
[14] D. A. Micha, J. Phys. Chem. **95**, 8082 (1991).
[15] D. Srivastava and D. A. Micha, Int. J. Quantum Chem. **QC-21**, 229 (1987).
[16] F. H. Mies and A. Giusti-Suzor, Phys. Rev. A **44**, 7547 (1991).
[17] B. R. Mollow, Phys. Rev. A **12**, 1919 (1975).

[18] K. F. Freed and A. A. Villaeys, J. Chem. Phys. **70**, 3071 (1979).
[19] R. J. Glauber, Phys. Rev. **98**, 1692 (1955).
[20] (a) W. H. Louisell, *Quantum Statistical Properties of Radiation* (Wiley, New York, 1973), Chap. V; (b) R. Loudon, *The Quantum Theory of Light* (Clarendon, Oxford, 1983), Chap. 8.
[21] M. Shapiro, J. Chem. Phys. **56**, 2582 (1972).
[22] B. W. Shore, Rev. Mod. Phys. **19**, 439 (1967).